Energy and Buildings 121 (2016) 32–42

Contents lists available at ScienceDirect

Energy and Buildings

journal homepage: www.elsevier.com/locate/enbuild

Application of artificial neural network for predicting hourly indoor air temperature and relative humidity in modern building in humid region

Leopold Mba[a,*], Pierre Meukam[b], Alexis Kemajou[a]

[a] Laboratory of Air Conditioning and Refrigeration, Advanced Teacher's Training College for Technical Education, University of Douala, PO Box 1872 Douala, Cameroon

[b] Laboratory of Energy, Water and Environment (L3E), National Advanced School of Engineering, University of Yaounde I, PO Box 8390 Yaounde, Cameroon

ARTICLE INFO

Article history:
Received 15 October 2015
Received in revised form 27 February 2016
Accepted 18 March 2016
Available online 1 April 2016

Keywords:
Building
Artificial neural network
Indoor air temperature
Relative humidity
Humid region
Matlab

ABSTRACT

The prediction of the air temperature (IT) and relative humidity (IH) in a building can help to reduce energy consumption for air conditioning. The purpose of this work was to apply the artificial neural network (ANNs) for an hourly prediction, 24–672 h in advance of (IT) and (IH) in buildings found in hot-humid region. The inputs used in the model are 12 last values of indoor and outdoor air temperature and relative humidity. The experimental building is built with cement hallow block in Douala-Cameroon. IT and IH were collected for 24 months. The experimental data were used to determine the optimal ANN structure with levenberg-marquardt algorithm using Matlab software. The optimal structure was the multilayer perceptron (MLP) with 36 input variables, 10 hidden neurons and two neurons in the output layer. The activation functions were respectively the hyperbolic tangent in the hidden layer and the linear function in the output layer. Moreover, the IT and IH results simulated by using the ANN model were strongly correlated with the experimental data, with the coefficient of correlation of 0.9850 for IT and 0.9853 for IH. These results testified that ANN can be used for hourly IT and IH prediction.

1. Introduction

Indoor thermal comfort conditions affect the amount of energy consumption in buildings [1,2] and they usually depend on the values of indoor air temperature and relative humidity [3]. The use of building energy simulation tools is an effective way in the estimation of the parameters of indoor thermal comfort. However, they necessitate several detailed input data such as properties of the building material, actual level of occupancy, energy produced by lights and equipment loadings [4]. Moreover, external unpredicted perturbations such as outdoor air temperature and relative humidity, soil temperature, radiation effects should also be taken into account [5]. The main barriers in using the current building simulation tools are the lengthy time required for simulations and complexity in the usage i.e. preparation of input data, execution and exploitation of results; unavailability and incompatibility of input data (weather conditions and the characteristics of building materials) [6]. Several techniques existing in literature reveal that nonlinear models are more effective than linear models for certain predictions [7]. As an easier alternative, the experimental data may be used to find out a black-box model or an empirical correlation defining the behavior of the thermal system. The limitation of this approach is that it requires assumption of the functional form of the proposed correlation [8]. The popular approach to analyze the steady and unsteady heat transfer problems is associated to the availability of non-linear empirical modeling methodologies, such as neural networks, inspired by the biological network of neurons in the brain [9–11]. Artificial neural networks (ANNs), which are increasingly being used in solving complex practical problems, are known as universal function approximators. They are capable of approximating any continuous nonlinear function to arbitrary accuracy [12]. Its applications are numerous in various fields including engineering, management, health, biology and even social sciences [13–17]. For the identification or analysis of heat transfer problems, a neural network approach has been attempted by many authors [18–20]. Singh et al. [21] used ANN for calculating thermal conductivity of rock. Various authors used neural networks for improved performance of built environment [22,23]. Alexiadis et al. [24] used ANN for the prediction of wind speed at six locations on the islands of the South and Central Aegean Sea in Greece. Some

* Corresponding author.
E-mail addresses: mba_leo@yahoo.fr, mblo20002002@yahoo.fr (L. Mba).

http://dx.doi.org/10.1016/j.enbuild.2016.03.046
0378-7788/

works were carried out on the prediction of surface air temperature in particular and other weather parameters by Njau [25,26].

Parishwad et al. [27] estimated the outdoor ambient temperature, relative humidity and air velocity in India using monthly–mean values of these parameters with developed correlations. The method can be used to predict the weather parameters at different locations of India.

Imran et al. [14] used ANN for the prediction of hourly mean values of outdoor ambient temperature 24 h in advance. This neural network is trained off-line using back propagation and batch learning scheme. The trained neural network was successfully tested on temperatures for years other than the one used for training. It requires a temperature value as input to predict the temperature of the following day for the same hour. Soleimani-Mohseni et al. [28] used nonlinear ANN models to estimate the operative temperature in a building by using other measurable variables, such as the indoor air temperature, electrical power use, outdoor temperature, time of the day, wall's temperature and ventilation flow rate. Lu and Viljanen [29] used an ANN model to predict either room air temperature or relative humidity. In that paper, the test house is a central ventilation control room. Measurements were taken from the test house in which indoor temperature and relative humidity were affected by ventilation machines. The experiment was carried for 30 days starting from January 2007. All the variables, temperatures and relative humidity indoor and outdoor, were collected within a 15 min interval. However, no outdoor relative humidity was available for outdoor temperatures below −10 °C. Satisfactory results with correlation coefficients 0.998 and 0.997 for indoor temperature and relative humidity were obtained in the testing stage. Mustafaraj et al. [30] investigates a neural network model to predict the indoor air temperature and relative humidity for the open-plan office positioned on the second floor in a modern commercial building in London. The data were collected for a period of nine months in the summer, autumn and winter seasons of 2005–2006 through the BMS's existing sensors. These data were used to build and validate the models. Kemajou et al. [31] predicted seven hours in advance the hourly indoor air temperature in modern building, by using an artificial neural network (ANNs) model, in hot-humid climate, using as inputs only the outdoor air temperature and the hourly values of indoor air temperature for the last six hours. The experimental building is built with cement hallow block in the town of Douala in Cameroon, and the experiment was carried out for six months. Similar works were carried out by Mba et al. [15]. Turkan et al. [3] predicted the daily mean indoor temperature (IT) and relative humidity values in an education building in Turkey by applying ANN. The city is located in a hot–humid region. The indoor air parameters, were collected between the 6th of June and 21st of September 2009, i.e. only for about four months via HOBO data logger. The R^2 values between predicted and actual values of indoor temperature and indoor relative humidity were computed as 0.94 and 0.96, respectively.

Despite the efforts these works made, very little studies have been carried out in the simultaneous prediction of the temperature and relative humidity in the literature. In hot and humid climate region, the most recent work was done by Turkan et al. [3]. This study was limited to a daily prediction of indoor air temperature and relative humidity, and authors used only four months of data collection in an experimental building. These data were used to build and validate the models.

In the present report, we present an ANN-based approach for predicting one day to one month in advance, the hourly indoor air temperature and relative humidity of a modern building with cement hallow block envelope in hot-humid climate region, using as input the last 12 hourly values of indoor air temperature and relative humidity, the last 12 hourly values of outdoor air relative humidity. Moreover, this study undertakes an overall analysis for a period of 24 months of the predictions of a room air temperature and relative humidity.

2. Material and methods

2.1. Climatic data of study area

The work is carried out in the town of Douala, the economic capital of the republic of Cameroon, situated in the heart of Africa. This town is about 24 km from the sea, on the left bank of the Wouri River and dominated by Mount Cameroon, West Africa's highest mountain (4095 m). Douala is located at 09°44 longitudes east and 04°01 latitude south. The height above the sea level is 5 m [32,33]. Average monthly data are collected over a period of nearly twenty years by the national meteorology of Cameroon [34]. Some data are presented on Fig. 1 below.

Fig. 1 shows the evolution of outdoor air relative humidity (a) and temperature (b). From Fig. 1a, monthly, the average of maximum relative humidity (OHmax) remains constant throughout the year and is approximately 97%, while the average of minimum relative humidity (OHmin) monthly varies between 59% and 77%. In Fig. 1b, the ambient air temperatures do not vary by an extreme amount. Monthly, the average maximum air temperatures during the day are between 28 °C and 33 °C and the average of daily minimum air temperature are between 23 °C and 24 °C. The highest of the monthly-mean maximum air temperatures reaches 33 °C in February and the lowest of the monthly-mean minimum air temperatures is 23 °C in August. Solar radiation is high. The annual global radiation reaches 4065 kWh/m^2 per day. The monthly average duration of sunshine collected between 1993 and 2013 varies between 68 h and 175 h [34]. The prevailing wind comes from the

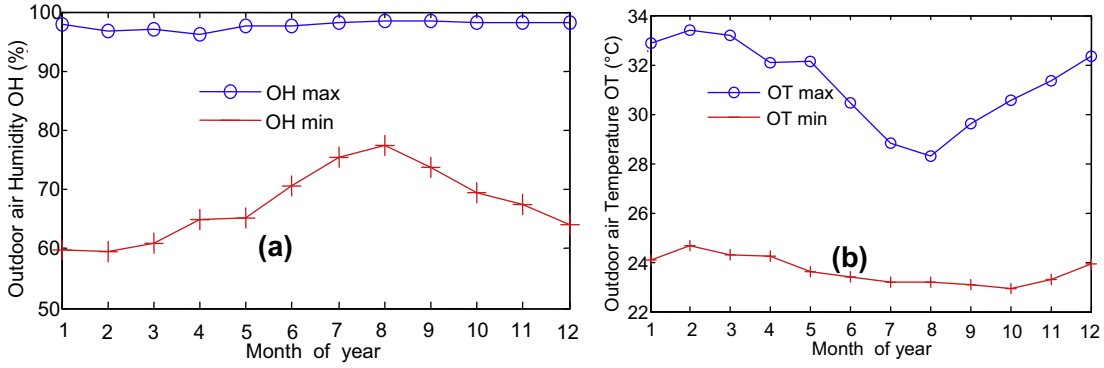

Fig. 1. Monthly average of outdoor air relative humidity and temperature.

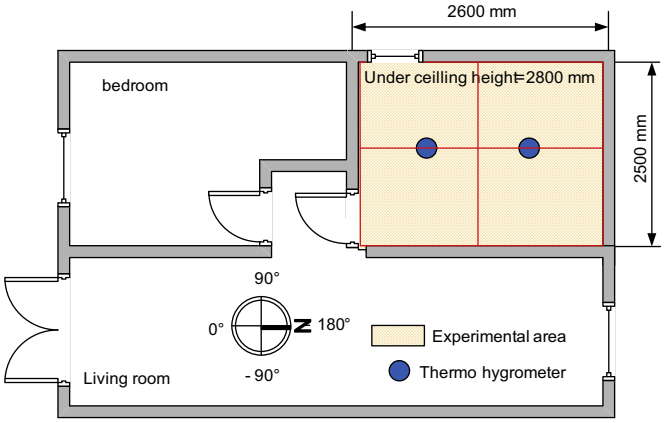

Fig. 2. Experimental building floor plan.

southwest. It blows mostly between 1.8 and 3.0 m per second. The rainfall reaches 4500 mm per year [31,34].

2.2. Experimental setup

It involves experimental building and data acquisition chain.

2.2.1. Experimental building

The measurements of indoor air temperature and relative humidity are carried out on a modern housing model built in 2007 (Fig. 2). The windows of 85 cm × 85 cm size, made of glass are operable but usually remain closed. Plank door with 190 cm × 85 cm size, opens into the living room. Building materials used for this housing are 15 cm thickness cement hallow concrete block with 2 cm thickness cement coating for an envelope, and 0.35 mm aluminium sheet for roofing, with a ceiling made of plywood. The ceiling height is 2.8 m. One room of 6.5 m^2 floor area is used to the experimentation from March 2010 to March 2013.

Instrumentation was used to record the indoor air temperature and relative humidity in the experimentation area.

2.2.2. Data acquisition chain

Data acquisition chain is the set of elements necessary to acquire, display, analyze and store data in the computer or export data to other applications. The data acquisition system measurement hardware may include a storage device for storing or subsequent use of the measurements. In this work, the data acquisition chain used to collect indoor air temperature and relative humidity data integrates a data logger.

The measuring apparatus was made of the following: a data acquisition apparatus called thermo hygrometers and a laptop computer. This thermo-hygrometer is the Reed Model C-342. The characteristics of the thermo hygrometers are presented in Table 1 below.

Two thermo hygrometers are installed at the experimental area. Indoor air temperature and relative humidity are simultaneously collected hourly, then processed and stored in the computer with the data acquisition system presented in Fig. 3.

In this figure, the steps of data acquisition and storage are presented. Fig. 3 shows the position of a thermo-hygrometer in the experimental space. This sensor is fixed to the ceiling with a wire. The height between the ground level and the sensor is more than 1.10 m and the distance between thermo-hygrometers and vertical walls varies from 0.86 m to 1.30 m. At this position, indoor air temperature and relative humidity data are recorded simultaneously and stored at the first time by a data logger integrated in the sensor unit. The last step in data acquisition chain is the display and data storage. To transfer data collected from thermo-hygrometers to the laptop, the RS- 232 cable is used. Using the SE-342 software installed in the machine, the communication is established between the sensors and the computer. The data are transferred, displayed and stored in the computer.

Table 1
Characteristics of temperature and relative humidity sensors.

Parameters	Temperature	Relative humidity
Range	−30 to 70 °C	0–100%
Resolution	0.1 °C	0.1%
Uncertainty	±0.4 °C	±3%

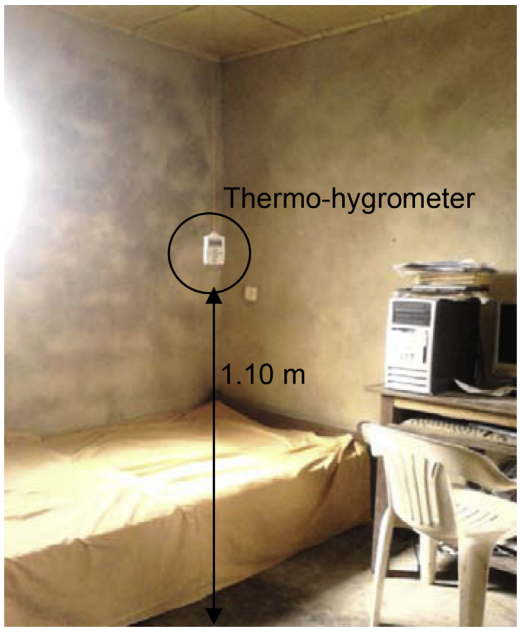

Fig. 3. Data acquisition chain.

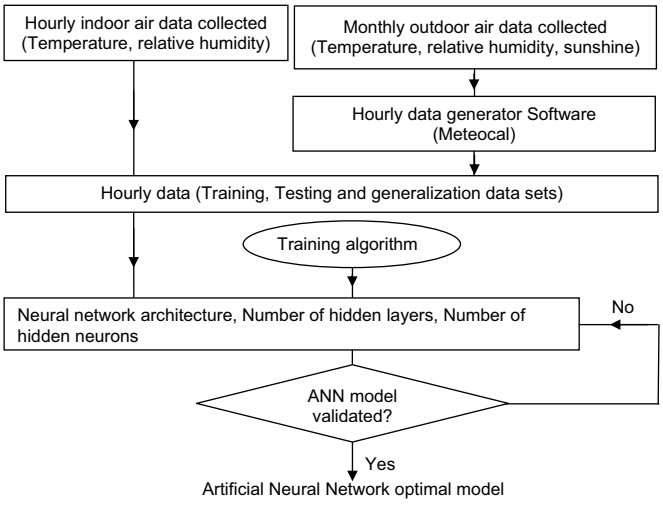

Fig. 4. Design method of an Artificial Neural Network model.

2.3. Design method of ANN model

The design of ANN model follows the method presented in Fig. 4 below.

According to this figure, the implementation of a neural network requires experimental database, neural network architecture, the training algorithm and learning process.

2.3.1. Experimental database

Coakley et al. [35], states that, in any modeling environment, the quality of results depends on that of the available inputs. To ensure the quality of the input data, outdoor air data are collected at the national meteorological service [34] over a period of 20 years. It is converted into hourly data with the help of MeteoCAL software and constitutes part of the model inputs. The second part of the model input data consists of indoor air data. They are collected over a period of 24 months with the thermo-hygrometers. Measurements of indoor air parameters were taken in accordance with ISO 7726 standard [36], at a height of 1.1 m from the ground level. This international standard is applied in many studies in the literature of thermal comfort [37,38].

Concerning the database for this work, the series of experimental values of the four characteristic quantities were collected, i.e. the outdoor and indoor air temperatures and relatives humidity. The yearly average air temperature and relative humidity recorded are presented in Fig. 5 below.

This figure shows the experimental database. The respective averages of outdoor air relative humidity OH, outdoor air temperature OT, indoor air relative humidity IH and indoor temperature IT are: 82.34%, 27.45 °C, 79.73% and 28.72 °C.

2.3.2. Artificial neural network structure

The structure of neuronal model consists of: the network architecture, the number of hidden layers and the number of hidden neurons.

The most widely used ANN architecture in prediction models is the multilayer perceptron (MLP) structure [11,15,17,31,39,40]. It has been proved that a MLP with a single hidden layer including a sufficient number of neurons can approximate any function with the desired accuracy [14,41]. Using two hidden layers rarely improves the model, and it may introduce a greater risk of converging to a local minima [48].

The MLP structure chosen consists of one hidden layer and an output layer. The input layer gathers the model's input vector x while the output layer yields the model's output vector y. The defining equation for the model is:

$$y(k) = f\left(y(k-1), y(k-2), \ldots, y(k-n_y), u(k-1), u(k-2), \ldots, u(k-n_u)\right) \quad (1)$$

where the next value of the dependent output signal $y(k)$, is regressed on previous values of the output signal and previous values of an independent input signal $u(k)$. n_y and n_u are the tapped delay lines TDL of output and input signals respectively. In this study, the input x is given by the hourly values of the vectors x_0 to $x_{n_y+n_u}$ listed in Table 2, and the output vector y consists of only one output vector. Each vector contains values of air temperature and relative humidity.

This Table presents input and output signals of the ANN model. Fig. 6 displays the one hidden layer MLP adopted for this work.

The hidden layer is characterized by several non-linear neurons. The non-linear function, i.e. the activation function is usually the tangent hyperbolic function $f(x) = \tanh(x)$. Therefore, an ANN with $(n_y + n_u + 1)$ inputs (see Table 2), h hidden neurons and a single output unit defines a non-linear parameterized mapping from an input x to an output y given by the following relationship:

$$y = y(x, w) = \sum_{j=0}^{h}\left[w_j \times f\left(\sum_{i=0}^{(n_y+n_u+1)} w_{ji}x_i\right)\right], \quad (2)$$

The parameters of the ANN model are given by the weights and biases that connect the layers between them. The ANN parameters, denoted by vector the parameter w, govern

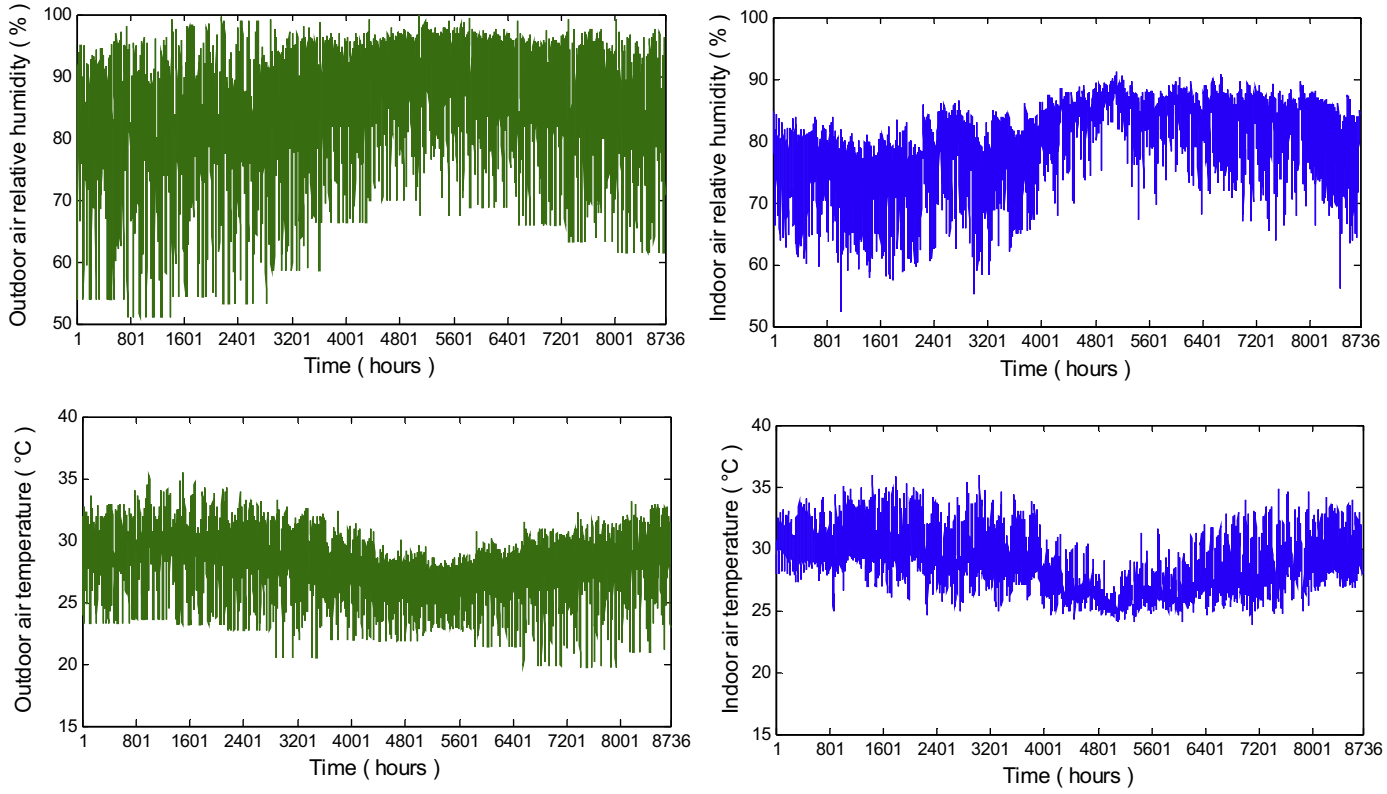

Fig. 5. Experimental average data for one year.

Table 2
Maximum input and output vectors of ANN model.

Variables	Description	
k		Hour
x_0	1	Bias
x_1	$u(k-1)$	Vector of previous values of outdoor air temperature OT and outdoor air relative humidity OH at time k – 1
x_2	$u(k-2)$	Vector of previous values of outdoor air temperature OT and outdoor air relative humidity OH at time k – 2
.	.	.
.	.	.
.	.	.
x_{n_u}	$u(k-n_u)$	Vector of previous values of outdoor air temperature OT and outdoor air relative humidity OH at time k – n_u
x_{n_u+1}	$y(k-1)$	Vector of previous values of indoor air temperature IT and indoor air relative humidity IH at time k – 1
x_{n_u+2}	$y(k-2)$	Vector of previous values of indoor air temperature IT and indoor air relative humidity IH at time k – 2
.	.	.
.	.	.
.	.	.
$x_{n_u+n_y}$	$y(k-n_y)$	Vector of previous values of indoor air temperature IT and indoor air relative humidity IH at time k – n_y
$y(k)$	[IT(k); IH(k)]	Vector of values of indoor air temperature IT and indoor air relative humidity IH at time k

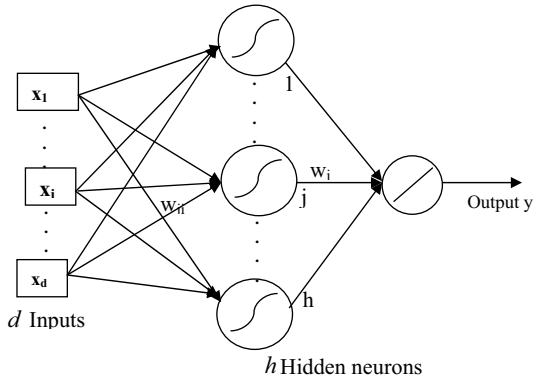

Fig. 6. Sketch of a MLP with d inputs and h hidden neurons.

the non-linear mapping. Parameters are estimated during the learning phase.

2.3.3. Learning, testing and generalization phases

There are three main steps to obtain the ANN optimal model: The learning, testing and generalization phases. During the learning phase, the ANN is trained using a training dataset of N inputs and output examples, pairs of the form $D = \{x_i, t_i\}_{i=1}^{N}$. The variable x contains samples of each of the $(n_y + n_u + 1)$ input vectors described in Table 1. The variable t, also called the target variable, is the corresponding measurement of the air relative humidity and temperatures.

This phase consist of adjusting w so as to minimize an error function J, which is usually the sum of the squares of the errors between the experimental output t_i and the ANN model output, $y_i = y(x_i; w)$:

$$J(w) = \frac{1}{2}\sum_{i=1}^{N}\{y_i - t_i\}^2 = \frac{1}{2}\sum_{i=1}^{N} e^2, \tag{3}$$

The learning algorithm used is the Levenberg-Marquardt. It is the fastest and ensures the best convergence to a minimum of mean square error (MSE) for function approximation problems [42–44]. The second and third phases are the testing and generalization phases. It consists of evaluating the ability of the ANN to replicate the observed phenomenon, that is to say, to give correct outputs when it is confronted with examples that were not seen during the training phase. Notice that during these phases, the testing and generalization dataset is used. Various statistical indices are proposed in the literature to check the predictive performance of models [42,43,45,46]. In this study, model performances are characterized by the mean square error (MSE) and the coefficient of correlation (R). MSE and R can be evaluated as:

$$MSE = \sum\left(\frac{e_i^2}{N}\right), \tag{4}$$

$$R = \pm\sqrt{\frac{\sum_{i=1}^{N}\left(y_i - \bar{t}\right)^2}{\sum_{i=1}^{N}\left(t_i - \bar{t}\right)^2}} = \pm\sqrt{1 - \frac{\sum_{i=1}^{N}(e_i)^2}{\sum_{i=1}^{N}\left(t_i - \bar{t}\right)^2}} \tag{5}$$

The realization of an ANN requires a fairly rigorous methodology. In order to achieve this, a simulation code was developed through Matlab software for learning.

3. Results and discussion

In order to evaluate the validity of the proposed approach, a real test scenario has been deployed. As mentioned previously, the literature revealed that ANNs is a useful tool to forecast daily indoor air temperature and relative humidity, with experimental data collected during four months. In this work, the prediction made by the ANN model is really relevant, because we want to forecast hourly indoor air temperature and relative humidity, 24 h and 168 h in advance with experimental data collected for 24 months. Experimental data consisting of hourly indoor air relative humidity (IH) and temperature (IT), outdoor air relative humidity (OH) and temperature (OT) values of a modern building found in hot-humid climate were collected: case of the town of Douala in Cameroon. The ANN model is trained with Levenberg-Marquardt algorithm software developed using Matlab. The trained model is used to forecast simultaneously hourly indoor air relative humidity and temperatures involving data other than those used for training. The developed model has been trained with 8736 experimental data pairs. Several MLP neural network structures are presented in Table 3 below.

Table 3 lists the MLP structure studied in this work. IT, IH, OT and OH represent indoor air temperature, indoor air relative humidity, outdoor air temperature and outdoor air relative temperature respectively.

3.1. ANN optimal structure

The criterion for choosing among these model architectures is the mean square error or the root mean square error on the test dataset.

Table 3
Input and output variables for each MLP structure studied.

Models	Outputs	Inputs	Description
M 1	$y(k)$	y(k − 1), y(k − 2), ..., y(k − 12), $u(k-1), u(k-2), ..., u(k-12)$	$y(k)$ = [IT(k); IH(k)] $u(k)$ = OH(k)
M 2	$y(k)$	y(k − 1), y(k − 2), ..., y(k − 12), $u(k-1), u(k-2), ..., u(k-12)$	$y(k)$ = [IT(k); IH(k)] $u(k)$ = OT(k)
M 3	$y(k)$	y(k − 1), y(k − 2), ..., y(k − 12), $u(k-1), u(k-2), ..., u(k-12)$	$y(k)$ = [IT(k); IH(k)] $u(k)$ = [OT(k); OH(k)]

Table 4
Testing performances of model M 1 for different test initialization parameters.

Hidden neurons	Mean square error (MSE) for test n°					Duration time
	1	2	3	4	5	
5	1.5932	4.4044	2.4404	3.1925	2.8064	3 min
10	1.4077	1.2901	1.3041	**0.7723**	2.5649	6 min
15	1.6989	0.8460	2.1899	1.9225	1.8409	8 min
20	2.1109	1.5061	1.2682	7.4114	1.9055	14 min

Bold values: represents the smallest value of the means square error of the model.

Table 5
Testing performances of model M 2 for different test initialization parameters.

Hidden neurons	Mean square error (MSE) for test n°					Duration time
	1	2	3	4	5	
5	2.5374	2.3425	1.4341	2.6177	2.9396	3 min
10	**0.7982**	2.5857	0.8541	1.5191	1.4694	7 min
15	1.4989	2.8842	1.9544	1.3788	1.2798	8 min
20	2.4822	1.1131	1.3221	0.9822	1.2800	13 min

Bold values: represents the smallest value of the means square error of the model.

Table 6
Testing performances of model M 3 for different test initialization parameters.

Hidden neurons	Mean square error (MSE) for test n°					Duration time
	1	2	3	4	5	
5	3.1399	7.6074	2.0805	2.9348	1.8422	4 min
10	0.9476	2.2177	1.0437	0.9394	2.3797	9 min
15	1.7208	1.5838	3.0124	1.1089	1.7821	14 min
20	1.0278	2.8880	2.0668	**0.9158**	2.8296	24 min

Bold values: represents the smallest value of the means square error of the model.

In order to model the experimental data, the number of hidden neurons for each ANN structure presented in Table 2 will be obtained by trial and error. So far, no mathematically justifiable method is available for determining the hidden elements. As explained by Haykin [47], training is started with a minimum number of elements. The number of these elements is constantly increased and re-training of the ANN is continued until satisfactory training is considered as the optimal number.

In this case, the mean-square errors (MSE) of the testing datasets of several examples of studied MLP neural network structures are calculated, and shown in Tables 4–6 .

3.1.1. *Effect of initialization parameters on model performances*

The analysis of mean-square error (MSE) in the Tables 4–6 shows the important effect of the initialization parameters, because for the same number of hidden neurons, MSE are different by varying the initialization of weights and biases.

3.1.2. *Effect of number of hidden neurons on simulation duration time*

The change in the number of neurons in the hidden layer of the artificial neural network ANNs model, has an impact on the duration of the simulation. Indeed, when the number of neurons increases, the simulation time increases also. In Tables 4–6, the number of hidden neurons increases from 5 to 20, when the simulation time change from 3 min to 14 min for the model M1, from

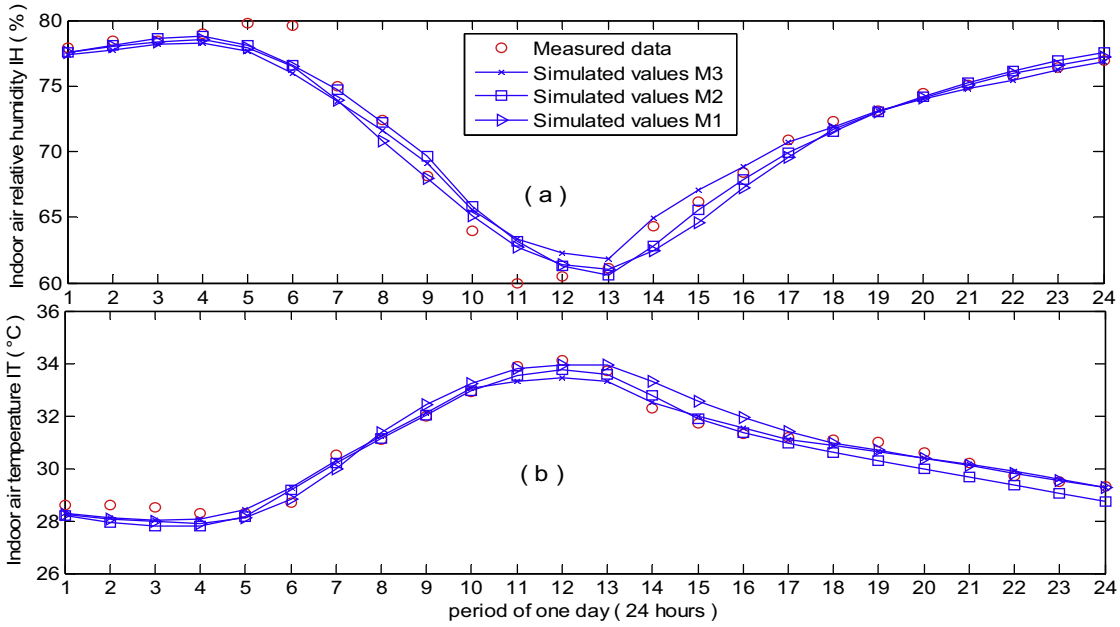

Fig. 7. Comparison of measured data and ANN simulated values of IT and IH for one day prediction.

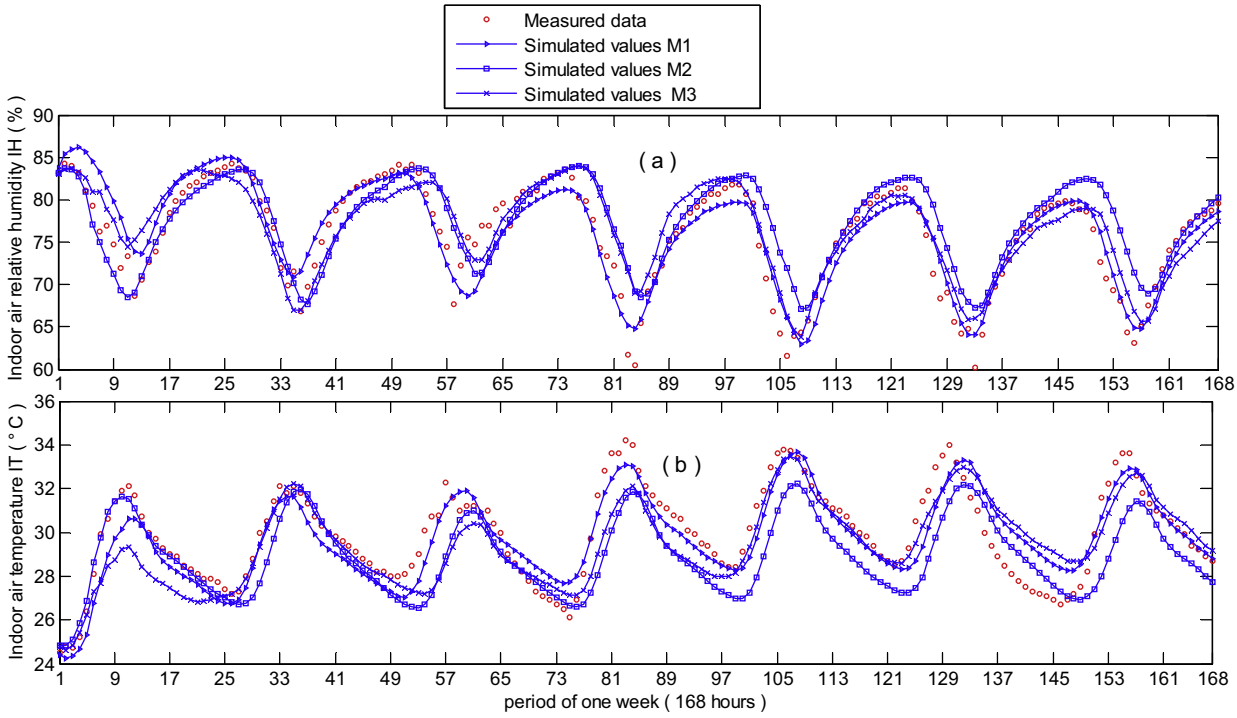

Fig. 8. Comparison of measured data and ANN simulated values of IT and IH for one week prediction.

3 min to 13 min for the model M2 and 4 min–24 min for the M3 model.

3.1.3. Effect of number of inputs on simulation time

Increasing model inputs causes an increase in the duration of the simulation. Analysis of Tables 4–6 show that the simulation times are almost identical for the models M1 and M2, and varies between 3–14 min. These two models have the same number of input variables, i.e., 36. The model M3, which has 48 input variables, has an average duration of simulation varying between 4 min and 24 min.

3.1.4. Effect of number of inputs on model performances

The analysis of Tables 4–6 shows a relationship between the number of input variables and the model performances.

Indeed, the structures of models M1 and M2 have the same input variables, i.e. 36, but the smallest values of mean square errors are 0.7723 and 0.7982 respectively. The model M3 with 48 input variables has it's smallest value of mean square errors of 0.9158, and therefore is the less efficient.

It means that when the input contains either outdoor air temperature or outdoor air relative humidity, the ANN structure is the best. But when it contains the outdoor air temperature and relative humidity, the ANN structure is the least efficient. In conclusion, it is useless to try to collect the two parameters for the simultaneous simulation of indoor air temperature and relative humidity in the building in a hot-humid region.

3.1.5. Performance comparison of different model structures

Table 4 shows the performances of the model M1, the input consists of the previous values of: indoor air relative humidity IH and temperature IT; and the outdoor air relative humidity OH. The lowest mean square error of 0.7723 and is observed in test No. 4. The number of hidden neurons is 10. Tests results performed with the model M2 were recorded in Table 5. The model has as inputs, the previous values of: indoor air temperatures IT and relative humidity IH; and outdoor air temperature OT. The minimum value of the mean square error recorded on the test No. 1 is 0.7982. The hidden layer also has 10 neurons. Tests carried out with the model M3 are recorded in Table 6. Previous values of indoor air temperature IT and relative humidity IH, outdoor air temperature OT and relative humidity OH constituted the inputs signal. Test No. 4, with 20 neurons in the hidden layer, has a minimum value of mean square error of 0.9158.

It appears from analysis that errors are minimized when the models M1 and M2 comprise 10 neurons in the hidden layer. For the M3 model, the error is minimal with 20 neurons in the hidden layer. MLP neural network structure with: 36 inputs, i.e. 12 previous values of indoor air temperature, 12 previous values of indoor air relative humidity and 12 previous values of outdoor air relative humidity; 10 hidden neurons with initial parameters corresponding to the test No. 4 of model M1, has the smallest mean square error MSE (0.7723) on the testing dataset. This model is the optimal model that allows the best approximation of the building's indoor air temperature IT and relative humidity IH.

Training phase is used to estimate the parameters, i.e. weights and biases of the models, and then to estimate the number of neurons in the hidden layer of each MLP structure studied. The test also eliminated the worst performing models. The final stage the generalization, done by the experimental validation of models.

3.2. Generalization phase

It consists of evaluating the ability of the ANN to give correct outputs when it is confronted with examples that were not seen during the training phase. At this stage, generalization dataset is used to validate experimentally the models.

During this phase, the ability of the models to predict IT/IH for a short and long term was tested, and the relationship between model performances and prediction period was found. The prediction periods chosen are: one day, one week and one month. The selection of these prediction periods (Figs. 7–9) was made randomly on the validation database and it does not influence the results.

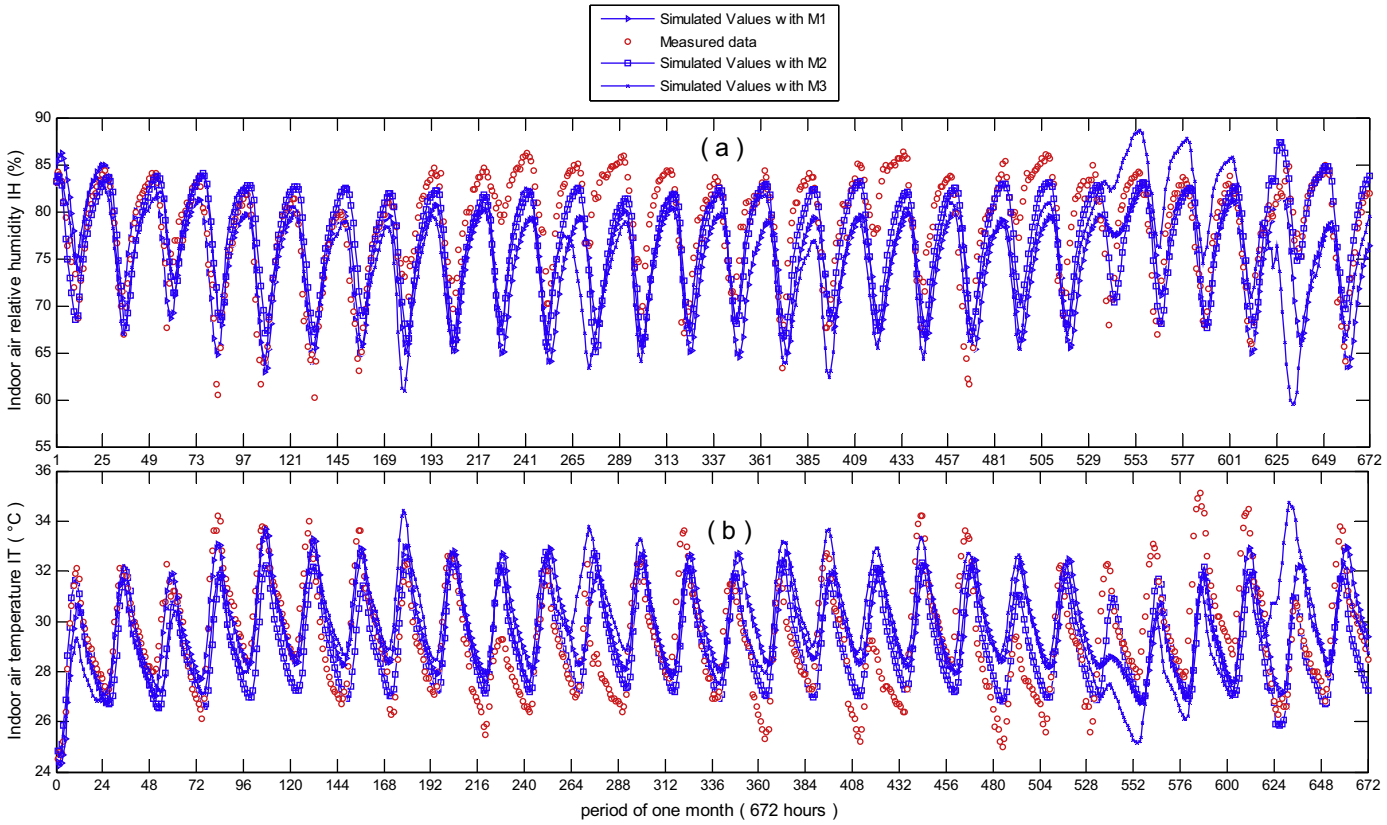

Fig. 9. Comparison of measured data and ANN simulated values of IT and IH for one month prediction.

The prediction must give the same results for another day, another week and one month, because, the parameters, i.e. weights and biases of the models are estimated during training phase. During this phase, the same estimated parameters are used.

One of the experimental validation criteria is a qualitative analysis. This analysis consists of a graphical comparison of the dynamic behavior of the simulated and measured data of indoor air temperature and relative humidity, in order to identify the dynamic differences.

3.2.1. Graphical validation

The comparison of ANN models' results and experimental results for indoor air temperature IT and indoor air relative humidity IH are shown in Figs. 7–9.

Fig. 7 presents the evolution of indoor air temperature and relative humidity simulated by the selected models and those measured in the experimental building. It permits to graphically compare simulated values to those measured. The results of graphical comparisons showed the strong similarities between experimental study and ANN model and supported the reliability of the model for a prediction 24 h in advance. The comparison of experimental values and simulation results for one week prediction is presented in the figure below.

Fig. 8 presents the comparison between experimental data and simulated values for different models. The evolution of relative humidity is similar to those of temperature in Fig. 7. It also shows that the models M2 and M3 present low correlation coefficients. Only the correlation coefficient of the M1 model is slightly high.

This figure presents the comparison between experimental data and simulated values for models M1, M2 and M3. Analysis of this figure shows a poor relationship between the measured and simulated values of IT and IH after 168 h of prediction.

According to Figs. 7 and 8, the estimated and experimental results are in a good agreement. This indicates that the obtained model can accurately estimate the indoor air temperature and relative humidity in a modern building in a humid climate. In Fig. 9, the deviation between experimental and ANN simulated values is very high and non-negligible for indoor air temperature IT and relative humidity IH.

The visual quality is however dependent on the display scale, and consequently, lack of objectivity. It gives an impression on the correlation between two variables without a precised idea of the intensity of the link. Another criterion that gives the intensity of the link between the simulated and measured values is calculated. This is the correlation coefficient R between the calculated values and those observed.

3.2.2. ANN efficiency

Linear regression between the model's response and the desired response is calculated. Figs. 10–12 show the regression lines between measured values and those simulated.

The straight regression lines between simulated and measured data are presented in the figures below. This method provides an additional indicator of quality which is the correlation coefficient R between y and x. This coefficient is equal to the ratio of the explained variance to the total variance of the output.

In these figures, we have for each response, a measured value and a simulated value. The respective notations measured and simulated values are: ITm and ITs for temperature, IHm and IHs for relative humidity of indoor air. The dotted line with a slope of 1 passing through the origin, is the equation for which the measured value is equal to the simulated value. If the model was perfect, all points would fall exactly on this line. It is therefore the distance

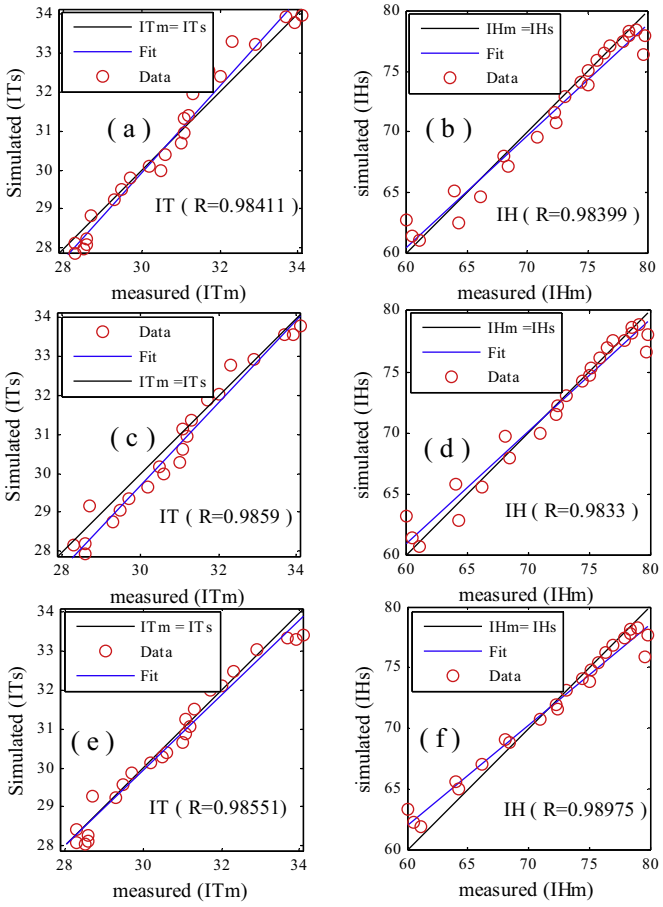

Fig. 10. Regression lines between measured values and values predicted one-day ahead.

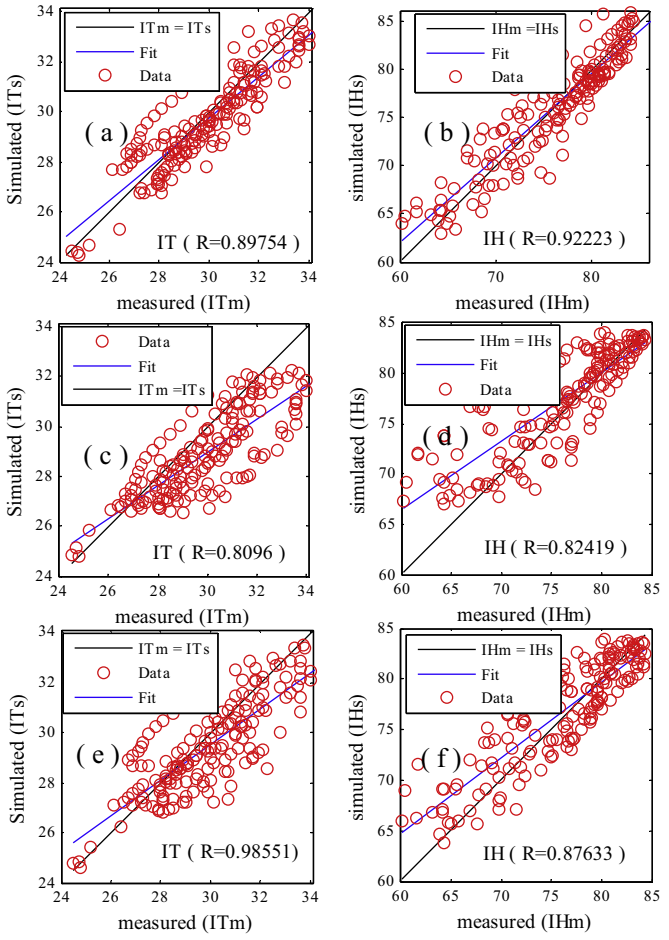

Fig. 11. Regression lines between measured values and values predicted one-week ahead.

between the points and the line which measures the error of the model.

The analysis of Figs. 10–12 highlighted several findings:

3.2.2.1. One-day-ahead prediction. For one-day-ahead prediction, the models M1 (Fig. 10a and b) and M2 (Fig. 10c and d), present the linear correlation coefficients for indoor air temperature higher than those of the indoor air relative humidity. This means that simulated values of indoor air temperature would adjust to the measured temperatures data better than those of indoor air relative humidity. Model M3 (Fig. 10e and f) has a linear correlation coefficients of indoor air relative humidity higher than those of temperature. Therefore, approximation of the relative humidity is improved compared to the temperature of the indoor air. The mean linear regression coefficients are respectively: 0.98405 for the model M1, 0.9846 for model M2 and 0.98763 for model M3. This means that the model M3 is more efficient than the model M2, which is also more efficient than the model M1. But the difference between these correlations coefficients is not significant. Other criteria such as the simulation time for each model, the horizon of prediction, can also influence the choice of the most efficient model.

3.2.2.2. One-week-ahead prediction. For the prediction of 168 h in advance, the models M1 (Fig. 11a and b), M2 (Fig. 11c and d) and M3 (Fig. 11e and f) have linear correlation coefficients of indoor air temperature lower than those of relative humidity.

According to this observation, the prediction of the relative humidity by the different models is improved in comparison to temperature.

The comparison of the measured values to those of the responses of models M1, M2 and M3 shows the respective average coefficient of linear correlation s of 0.9098, 0.8168 and 0.8429. According to the results, the model M1 gives the best approximation of the couple of indoor air temperature and relative humidity, followed by the model M3.

3.2.2.3. One-month-ahead prediction. For the prediction of one month in advance, the models M1 (Fig. 12a and b), M2 (Fig. 12c and d) and M3 (Fig. 12e and f) have the linear correlation coefficients of the indoor air temperature lower than those of relative humidity.

The comparison of the measured values to those of the responses of models M1, M2 and M3 shows the respective average coefficient of linear correlations of 0.6295, 0.7037 and 0.5193. According to the results, the model M2 gives the best approximation of the couple of indoor air temperature and relative humidity. The worst model for one month prediction is M3, with a R of 0.5193.

The averages of linear correlation coefficients of models M1, M2 and M3, for the periods of one day to one week of prediction are respectively 0.947, 0.913 and 0.90. This allows that, the model which provides the best approximation of indoor air temperature and the relative humidity in modern building built with cement hollow block in hot and humid climate is the model M1. For the short-term forecast for the periods of 1–24 h and 1–168 h ahead, the

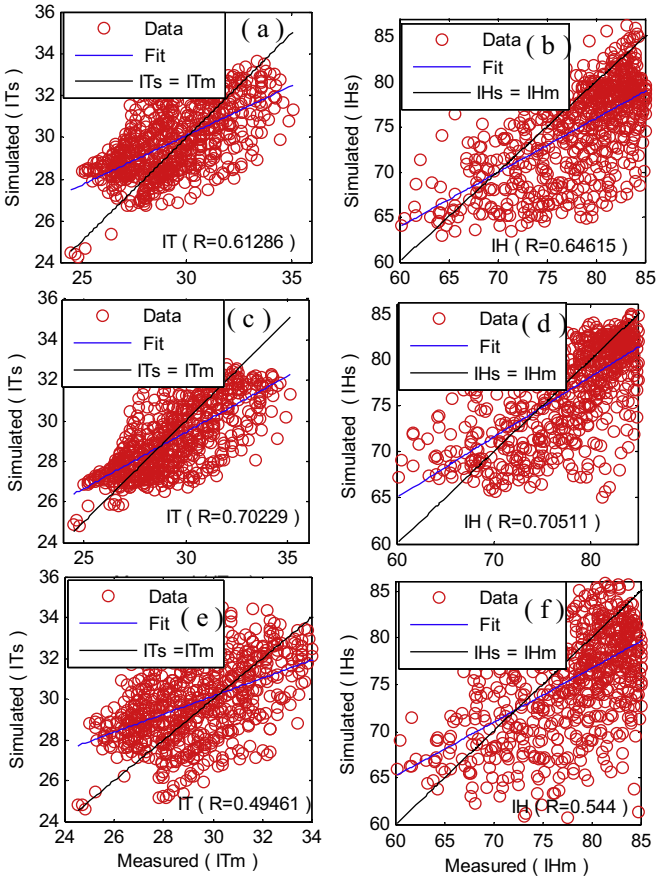

Fig. 12. Regression lines between measured values and values predicted one-month ahead.

average of linear correlation coefficient for all models are respectively: 0.985 and 0.833 for indoor air temperature; 0.9853 and 0.874 for indoor air relative humidity.

3.2.3. *Validation of results with other similar works*

According to the analysis done in this work, the simulated values of indoor air relative humidity are adjusted to the measured values better than those of indoor air temperature in modern building, and the linear correlation coefficients vary between 0.809 and 0.989. Buratti et al. [16] used ANN-models to estimate indoor air temperature, and the obtained value of linear correlation coefficient is 0.9625. In the works of Paudel et al. [40], the R-value evaluated on the test database varies between 0.61 and 0.85. Turkan et al. [3] estimated daily indoor air temperature and relative humidity in Turkey, and linear correlation coefficients are 0.94 for temperature and 0.96 for relative humidity. Lu and Viljanen [29] used an ANN model to predict either room air temperature or relative humidity, satisfactory results with correlation coefficients 0.998 and 0.997 for indoor temperature and relative humidity respectively were obtained.

4. Conclusion

This paper presents an ANN models used for the prediction of indoor air temperature and relative humidity, 24 h and one month in advance, for a modern building in humid climate, using as inputs the 12 previous outdoor air relative humidity, and the 12 last hourly values of indoor air temperature and relative humidity. The results of this investigation show that ANN can effectively model. It is understood that, ANN can be used for modeling of indoor air temperature IT and relative humidity IH. The biggest advantages of the ANN compared to classical methods are speed of calculations and capacity to learn from examples. In addition, in the domain of buildings, the proposed model, compared to others does not require any thermodynamic properties of building materials, solar flux, wind speed, etc. Experimental data were compared with result obtained from ANN and all data were analyzed statistically. When analyses were assessed, the values of results obtained from ANN was very close to the values of experimental results and therefore, it was seen that the ANN might be used safely. The obtained results were also compared with other similar works. ANN as an alternative method can be used to estimate the indoor air temperature and relative humidity of the building.

References

[1] R. Holz, A. Hourigan, R. Sloop, P. Monkman, M. Krarti, Effects of standard energy conserving measures on thermal comfort, Build. Environ. 32 (1) (1997) 31–43.
[2] K.W. Tham, M.B. Ullah, Building energy performance and thermal comfort in Singapore, ASHRAE Trans. 99 (1) (1993) 308–321.
[3] Turkan Goksal Ozbalta, Alper Sezer, Yusuf Yıldız, Models for prediction of daily mean indoor temperature and relative humidity: education building in Izmir, Turkey, Indoor Built Environ. 21 (6) (2012) 772–781.
[4] T. Catalina, J. Virgone, E. Blanco, Development and validation of regression models to predict monthly heating demand for residential buildings, Energy Build. 40 (2008) 1825–1832.
[5] N. Mendes, G.H.C. Oliveira, H.X. Araujo, L.S. Coelho, A Matlab-based simulation tool for building thermal performance analysis, in: Eighth International IBPSA Conference, Eindhoven, Netherlands, 2003, 8 p.
[6] Papamicheal Konstantinos, Pal Vineeta, Barriers in developing and using simulation-based decision-support software, in: Presented at the ACEEE 2002 Summer Study on Energy Efficiency in Building, August 18–23, and published in the proceedings, 2002, 5 p.
[7] R.H. Dodier, G.P. Henze, Statistical analysis of neural networks as applied to building energy prediction, Trans. ASME 126 (1) (2004) 592–600.
[8] Rakoczy Masiuk, Application of artificial neural network to assessment of influence of operational parameters on the characteristic quantities of thermal transient process in a reciprocating mixer, in: 5th European Thermal-Sciences Conference, the Netherlands, 2008, 8 p.
[9] Tawfiq Al-Saba, Ibrahim EI-Amin, Artificial neural networks as applied to long-term demand forecasting, Artif. Intell. Eng. 13 (1999) 189–197.
[10] H. Huang-Chu, H. Rey-Chue, Jer-guang Hsieh, A new artificial peak power load forecaster based on non fixed neural networks, Electr. Power Energy Syst. 24 (2001) 245–250.
[11] Mba Léopold, Modélisation du comportement thermique du bâtiment: application d'une méthode neuronale. Université de Douala-Cameroun, mémoire de DEA présenté au laboratoire d'énergie de l'école doctorale des Sciences Fondamentales et Appliquées, 2009, 68 p.
[12] G. Cybenko, Approximation by superposition of a sigmoidal function, Math. Control Signal Syst. 2 (1989) 303–314.
[13] Bauer Manuel, Gestion biomimétique de l'énergie dans le bâtiment. Ecole Polytechnique Fédérale de Lausanne. Thèse de doctorat présentée d'architecture, 1998, 189 p.
[14] Imran Tasadduq, Shafiqur Rehman, Khaled Bubshait, Application of neural networks for the prediction of hourly mean surface temperatures in Saudi Arabia, Renew. Energy 25 (2002) 545–554.
[15] Mba Léopold, A. Kemajou, P. Meukam, Application of artificial neural network for modeling the thermal behavior of building in humid region. In Formation, recherche, innovation et développement au cœur de l'interdisciplinarité. Actes des 3ème rencontres EG@ Yaoundé, Cameroun, 14–16 septembre 2010. L'Harmattan, 2012, pp. 168–184.
[16] Cinzia Buratti, Elisa Lascaro, Domenico Palladino, Marco Vergoni, Building behavior simulation by means of artificial neural network in summer conditions, Sustainability 6 (2014) 5339–5353.
[17] Valerio Lo Brano, Giuseppina Ciulla, Mariavittoria Di Falco, Artificial neural networks to predict the power output of PV panel, Int. J. Photoenergy 2014 (2014) 1–12, Article ID 193083.
[18] J. Thibault, B.P.A. Grandjean, A neural network methodology for heat transfer data analysis, Int. J. Heat Mass Transfer 34 (1991) 2063–2070.
[19] G.J. Zdaniuk, Heat Transfer and Friction in Helically-finned Tubes Using Artificial Neural Networks. Ph.D. dissertation, Mississippi State University, 2006.
[20] S. Yilmaz, K. Atik, Modeling of a mechanical cooling system with variable cooling capacity by using artificial neural network, Appl. Therm. Eng. 27 (2007) 2308–2313.
[21] T.N. Singh, S. Sinha, V.K. Singh, Prediction of thermal conductivity of rock through physic-mechanical properties, Build. Environ. 42 (2007) 146–155.
[22] J.F. Kreider, Neural networks applied to building energy studies, in: H. Bloem (Ed.), Workshop on Parameter Identification, JRC Ispra, Ispra, 1995, pp. 243–251.

[23] Subodh Kumar Sinha, Manju Rani, Gayatri, P.K. Mandal, Expression pattern analysis of different micro RNAs under nitrogen deprivation condition in root tissues of different wheat genotypes, Indo Global J. Pharm. Sci. 4 (3) (2014) 194.
[24] M.C. Alexiadis, P.S. Dokopoulos, H.S. Sahsamanoglou, I.M. Manousarids, Short-term forecasting of wind speed and related electrical power, Sol. Energy 63 (1) (1998) 61–69.
[25] E.C. Njau, Prediction of meteorological parameters: I. Analytical method, Nuovo Cimento 14C (1991) 473–488.
[26] E.C. Njau, Prediction of meteorological parameters: II. Methods based on an electronic system, in: Proceedings of the International Conference on Global Warming and Climate Change, Geneva, Switzerland, 1993.
[27] G.V. Parishwad, R.K. Bhardwaj, V.K. Nema, Prediction of monthly-mean hourly relativehumidity, ambient temperature, and wind velocity for India, Renew. Energy 13 (3) (1998) 363–380.
[28] M. Soleimani-Moheseni, B. Thomas, Fahien Per, Estimation of operative temperature in buildings using artificial neural networks, Energy Build. 38 (2006) 635–640.
[29] Tao Lu, Martti Viljanen, Prediction of indoor temperature and relative humidity using neural network models: model comparison, Neural. Comput. Appl. 18 (2009) 345–357.
[30] G. Mustafaraj, J. Ghena, G. Lowry, Thermal behaviour prediction utilizing artificial neural networks for an open space, Appl. Math. Model. 34 (2010) 3216–3230.
[31] Alexis Kemajou, Léopold Mba, Pierre Meukam, Application of artificial neural network for predicting the indoor air temperature in modern building in humid region, Br. J. Appl. Sci. Technol. 2 (1) (2012) 23–34.
[32] A. Mélingui, M. Gwanfogbe, J. Nguoghia, J. Mounkam, Nouvelle Géographie du cameroun 3ème, EDICEF (1987) 120 Pages.
[33] A. Mélingui, M. Kuete, J. Nguoghia, J. Mounkam, D. Nofiole, Nouvelle Géographie 3ème, Nouvelle édition, EDICEF, 1993.
[34] Météo, Météorologie Nationale du Cameroun, Tableaux Climatologiques Mensuels TCM. Direction Nationale de la météorologie. Douala, Cameroun, 2014.
[35] Daniel Coakley, Paul Raftery, Marcus Keane, A review of methods to match building energy simulation models to measured data, Renew. Sust. Energy Rev. 37 (2014) 123–141.
[36] ISO 7726, Ergonomics of the Thermal Environment—Instruments of Measuring Physical Quantities, International Organization for Standardization, Geneva, 1998.
[37] Modeste Kameni Nematchoua, Rene Tchinda, Wagner Augusto Andreasi, Noel Djongyang, Adaptive study of thermal comfort in equatorial zone: case of some buildings in Cameroon, Int. J. Emerging Technol. Adv. Eng. 4 (2) (2014) 36–47, www.ijetae.com (ISSN 2250-2459, ISO 9001:2008, Certified Journal).
[38] Erick Johansson, Sofia Thorsson, Rohinton Emmanuel, Eduardo Kruger, Instruments and methods in outdoor thermal comfort studies—the need for standardization, Urban Clim. 10 (2014) 346–366.
[39] T. Manssouri, H. Sahbi, I. Manssouri, B. Boudad, Utilisation d'un modèle hybride base sur la rlms et les rna-pmc pour la prédiction des paramètres indicateurs de la qualité des eaux souterraines cas de la nappe de Souss-Massa-Maroc, Eur. Sci. J. 11 (June) (2015) 35–46.
[40] Subodh Paudel, Mohamed Elmtiri, Wil L. Kling, Olivier Le Corre, Bruno Lacarrière, Pseudo dynamic transitional modeling of building heating energy demand using artificial neural network, Energy Build. (2014), http://dx.doi.org/10.1016/j.enbuil.2013.11.051.
[41] S.A.M. Said, Degree-day base temperature for residential building energy prediction in Saudia Arabia, ASHRAE Trans. Res. 98 (1) (1992) 346–353.
[42] D. Dreyfus, J.M. Martinez, M. Samuelides, M.B. Gordon, F. Badran, S. Thiria, L. Hérault, Réseaux de neurones, méthodologie et applications, 2ème édition, Eyrolles, 2002.
[43] Howard Demuth, Mark Beale, Martin Hagan, Neural Network Toolbox 5: User's Guide. Guide d'utilisation des réseaux de neurones sur le logiciel Matlab, 2007.
[44] Chaabani, Modélisation du procédé d'hydrotraitement du gasoil à l'aide des réseaux de neurones artificiels. Université m'hamed bougara boumerdes. Mémoire de fin d'études présenté en Faculté des Hydrocarbures et de la Chimie. Algérie, 2008, 128 p.
[45] S. Jassar, Z. Liao, L. Zhao, Adaptive neuro-fuzzy based inferential sensor model for estimating the average air temperature in space heating systems, Build. Environ. 44 (2009) 1609–1616.
[46] J.P. Corriou, Les réseaux de neurones pour la modélisation et la conduite des procédés. Lavoisier Technique et Documentation. Paris-France, 1995.
[47] S. Haykin, Neural Networks: A Comprehensive Foundation, Prentice Hall, Upper Saddle River, NJ, 1994.
[48] G. Panchal, A. Ganatra, Y.P. Kosta, D. Panchal, Behaviour analysis of multilayer perceptrons with multiple hidden neurons and hidden layers, Int. J. Comput. Theory Eng. 3 (2) (2011) 332–337.